Available online at www.sciencedirect.com
ScienceDirect
Journal of Nuclear Materials 374 (2008) 87–94
journal of nuclear materials
www.elsevier.com/locate/jnucmat

Structure and properties of vacancy and interstitial clusters in α-zirconium

N. de Diego [a,*], Yu.N. Osetsky [b], D.J. Bacon [c]

[a] Dpto. de Física de Materiales, Facultad de Ciencias Físicas, Universidad Complutense, Ciudad Universitaria, 28040 Madrid, Spain
[b] Computer Science and Mathematics Division, ORNL, Oak Ridge, TN 37831, USA
[c] Materials Science and Engineering, Department of Engineering, The University of Liverpool, Liverpool L69 3GH, UK

Received 29 January 2007; accepted 20 July 2007

Abstract

The structure and properties of planar interstitial and vacancy clusters in α-zirconium containing up to ≈300 defects were studied by atomic-scale computer modelling. Clusters of different shape and habit plane have been simulated at zero temperature. Vacancy clusters were constructed as close-packed platelets of vacancies in (0001), $\{11\bar{2}0\}$ and $\{1\bar{1}00\}$ planes. Clusters of self-interstitial atoms were formed as planar arrays of $\langle 11\bar{2}0\rangle$ crowdions (the most stable configuration for the model potential used) in a $\{11\bar{2}0\}$ plane. The most favourable shape for both types in the $\{11\bar{2}0\}$ and $\{1\bar{1}00\}$ prism planes is rectangular and clusters relax to perfect dislocation loops with Burgers vector $\boldsymbol{b} = 1/3\langle 11\bar{2}0\rangle$. Their stability is increased by dissociation of the sides in basal planes. Vacancy clusters in the (0001) basal plane form hexagonal loops enclosing an extrinsic stacking fault with $\boldsymbol{b} = 1/2[0001]$. Quantitative information is provided on the energy and structure parameters of the clusters.

1. Introduction

Zirconium (Zr) and its alloys play an important role in nuclear industry and have been studied extensively by experimental and theoretical techniques. However, new approaches to create predictive tools based on multi-scale modelling require detailed information on material properties, especially in the length and time ranges where theoretical models cannot be applied. Particular problems arise in the description of point defects and their clusters, for their evolution and reactions with other microstructure features determine the accumulation of radiation damage and radiation effects.

Much work has been devoted to the study of point defect clusters in cubic metals in recent years [1–4] but, despite the relevance of zirconium for nuclear technology, a comprehensive analysis of the morphology and properties of point defect clusters is not yet available for hcp metals. After the extensive review by Bacon in 1988 on point defects and point defect clusters in hcp metals [5], little attention has been paid to this subject. Kapinos et al. [6] performed static simulations of vacancy platelets in Zr on (0001) and $\{10\bar{1}0\}$ planes, concluding that the most favourable energetically are vacancy clusters with dislocation loop character $\frac{1}{2}[0001](0001)$ and $\frac{1}{2}[10\bar{1}0]\{10\bar{1}0\}$. More recently, Kulikov and Hou [7] studied the morphology and thermal stability of voids and vacancy loops in Zr and found that the formation energy of voids is smaller than that of vacancy loops. Small vacancy clusters have been also identified in molecular dynamics simulation of displacement cascades [8–11]. As far as self-interstitial atom (SIA) clusters in Zr are concerned, de Diego et al. [12] investigated the properties and mobility of small clusters, concluding that the most stable ones are formed in the $\{11\bar{2}0\}$ type-II prism planes. Cascade simulation by computer has demonstrated that this type of SIA cluster is

* Corresponding author. Tel.: +34 913944489; fax: +34 913944547.
E-mail address: nievesd@fis.ucm.es (N. de Diego).

0022-3115/$ - see front matter © 2007 Elsevier B.V. All rights reserved.
doi:10.1016/j.jnucmat.2007.07.011

formed in the primary damage state in Zr [9,10]. More recent studies on defect cluster formation in displacement cascades have identified two more types: a triangular cluster formed by up to six SIAs in the basal plane and an irregular 3D arrangement extended along the *c*-axis [11].

In this work we present results of atomic-scale computer modelling of the structure and stability of the most stable vacancy and SIA clusters in Zr. Section 2 describes the method and defect construction. The results for SIAs and vacancies are presented and discussed in Sections 3.1 and 3.2, respectively, and compared with experiment in Section 3.3. The conclusions are summarised in Section 4.

2. Computational method and cluster construction

The cluster configurations and properties have been studied by simulating model crystallites using static modelling, i.e. simulation of 0 K, by potential energy minimisation. The crystallites of parallelepiped shape contained between 15,000 and 100,000 mobile atoms, depending on the defect size and shape. A combination of conjugate gradients and quasi-dynamical relaxation was used to relax the defect configuration, as described previously [1–4]; fixed boundary conditions were used. The interatomic interactions were described by the many-body potential developed by Ackland et al. [13] for zirconium.

The vacancy clusters were created in the crystallite centre in either the (0001) basal plane or the $\{1\bar{1}00\}$ type-I or $\{11\bar{2}0\}$ type-II prism planes (PPI and PPII in the following). The shapes considered are those with the lowest energy. The basal-plane defects were generated by removing atoms in one (0001) atomic plane from regions with a regular hexagonal shape bounded by $\langle 11\bar{2}0\rangle$ sides. For the clusters in the prism planes the atoms were removed from areas of rectangular shape in two adjacent atomic planes, i.e. one plane of the lattice. Two sides of the rectangle were in the *c*-axis direction [0001] and the other two were in the basal plane (0001). Different shape factors were considered by changing the ratio of the length of the rectangle sides, $f = h/l$, where h is the size along the *c*-axis and l is the size in the basal plane along either $\langle 11\bar{2}0\rangle$ or $\langle 10\bar{1}0\rangle$ directions for clusters in the PPI or PPII planes, respectively.

The SIA clusters were constructed from the most stable SIA configuration for the potential model used, which is a $\langle 11\bar{2}0\rangle$ crowdion in the basal plane [13]. The arrangement of four interstitials depicted in Fig. 1 shows the basic unit used to build the SIA clusters in the PPII. This 4-SIA cluster has been found to be the most stable among all the possible four-interstitial configurations in Zr [12]. It is equivalent to the introduction of four closely-packed $[\bar{1}2\bar{1}0]$ crowdions in the two adjacent $(\bar{1}2\bar{1}0)$ planes. The SIA clusters in the PPII were created in the crystallite centre in the $(\bar{1}2\bar{1}0)$ plane by stacking four closely-packed interstitials along the $[10\bar{1}0]$ and [0001] directions. Several cluster shapes have been considered, i.e., rectangle, rhombus and hexagon. For the rectangular clusters different

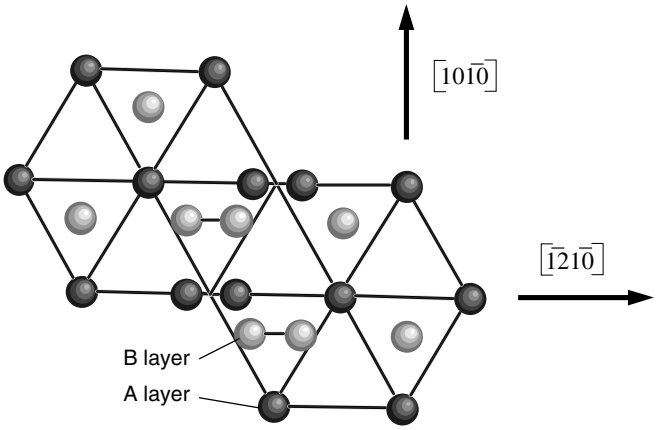

Fig. 1. Configuration of the 4-SIA cluster considered as a basic unit to form larger clusters. The scheme shows a basal plane projection in which the interstitials are represented as two spheres sharing a regular position of the hcp lattice. Dark and light symbols denote A- and B-type layers, respectively.

shape factors, f, were considered by changing the cluster dimensions along the [0001] and $\langle 10\bar{1}0\rangle$ directions, as described above for vacancies.

The binding and formation energies of the extended clusters have been calculated and the final structure analysed by studying appropriate cluster cross-sections. Moreover, the distribution of the density of Burgers vector, $\rho(b) = \Delta u_x/\mathrm{d}x$, in the planes that form the cluster glide cylinder has been studied to determine the possible dislocation character of the cluster. Here Δu_x is the displacement difference between neighbouring atoms across the slip plane, i.e. glide cylinder surface, and x is the direction of the cylinder axis, i.e. $\boldsymbol{b}$.

To check the thermal stability of the clusters we used molecular dynamics: the relaxed crystallite was heated to about 700 K and annealed for times up to 600 ps and then relaxed again at 0 K to the minimum potential energy.

3. Results and discussion

3.1. SIA clusters

Clusters containing from 8 to 288 SIAs in the $\{\bar{1}2\bar{1}0\}$ plane were simulated. Smaller clusters have been described elsewhere [12] and will not be considered here. Different shapes have been studied: rectangle with the longest side along either [0001] or $\langle 10\bar{1}0\rangle$ direction, rhombus with edges along $\langle 10\bar{1}1\rangle$ directions, and hexagon, which can also be described as rhombus with truncated vertices on the basal plane. For the rectangular defects shape factors in the range $0.30 \leqslant f \leqslant 1.38$ have been studied.

Cluster formation, E_f, and binding energy, E_b, normalised by the total number of defects in the cluster, n, are plotted as a function of n in Fig. 2. The formation energy 3.756 eV of the single $\langle 11\bar{2}0\rangle$ crowdion has been taken as a reference in calculating E_b. The changes in E_b with n and cluster shape reflect those in E_f. It can be seen that rect-

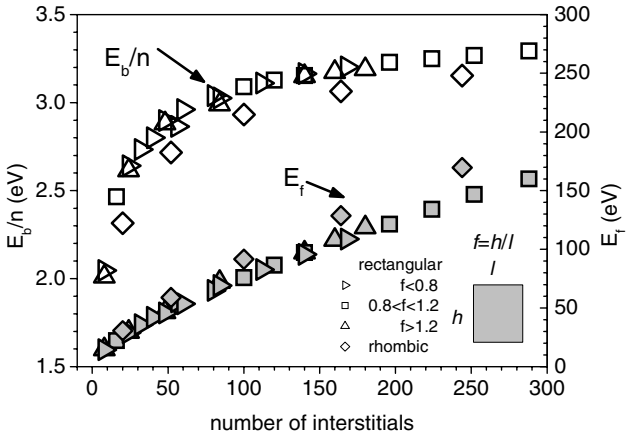

Fig. 2. The formation and binding energies per interstitial of SIA clusters versus the number of interstitials n. The clusters were created in the PPII plane. Only data for the rectangular and rhombic clusters are plotted.

angular clusters are the most stable and rhombus-shaped ones have the lowest binding energy. The hexagons in the PPII have binding energy that falls between that for the rectangles and rhombi but the values have not been plotted for the sake of clarity. The binding energy increases with cluster size, irrespective of the cluster shape and the shape factor value, f. In fact, it is seen in the figure that the shape factor has little influence on the formation energy.

The structure has been studied by analysing the atomic positions through the cluster centre in $[1\,0\,\bar{1}\,0]$ and $[0\,0\,0\,1]$ projections. The general finding for all the clusters in the PPII is that they have features of dislocation loops. In order to characterise the dislocation core forming the sides of a cluster, the distribution of Burgers vector, $\rho(b)$, in the $[\bar{1}\,2\,\bar{1}\,0]$ direction on the $(0\,0\,0\,1)$ and $(1\,0\,\bar{1}\,0)$ planes of the glide prism has been determined for each cluster. To study the structure of the core segment on the basal plane, the difference in the atomic displacements was calculated between two atomic rows separated by the $(0\,0\,0\,1)$ plane through the cluster side; we label these pairs of rows Bm, where m specifies the row number. Similarly, for the dislocation segment lying on the $(1\,0\,\bar{1}\,0)$ plane, the displacement

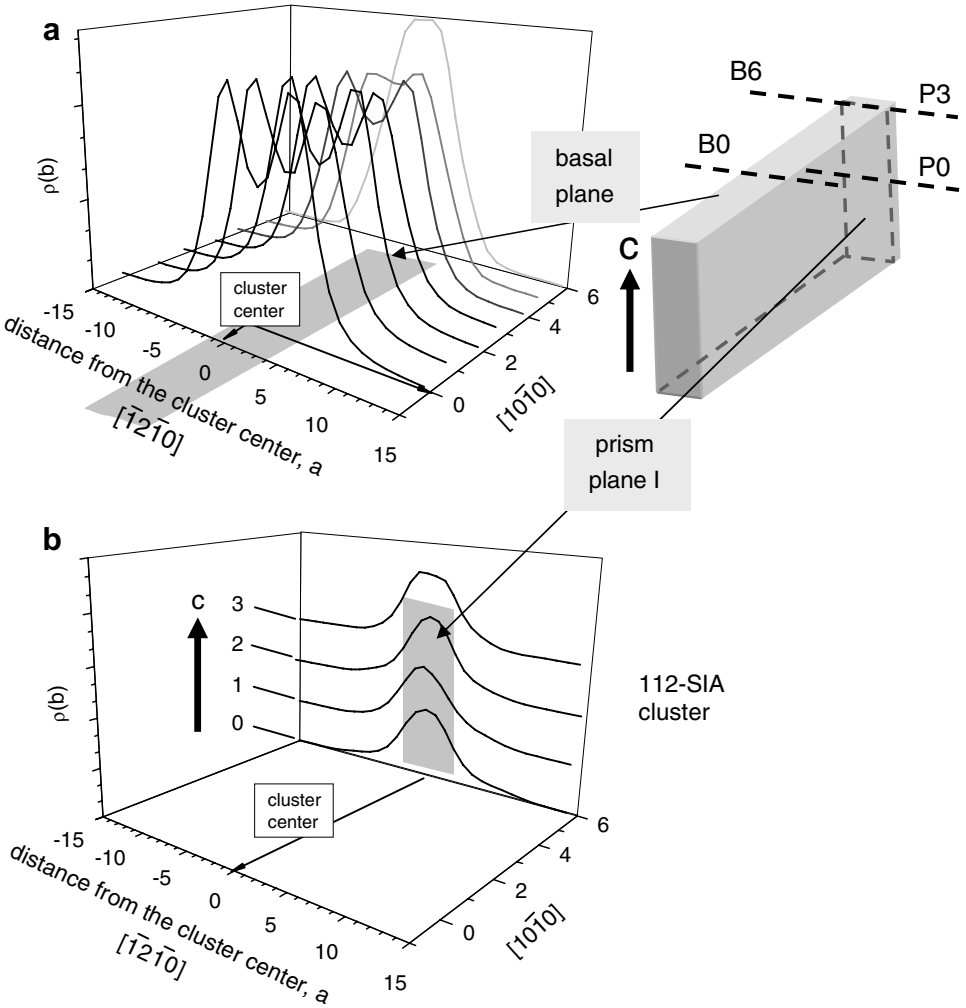

Fig. 3. The Burgers vector density $\rho(b)$ for segments in (a) $(0\,0\,0\,1)$ and (b) $(1\,0\,\bar{1}\,0)$ planes for a 112-SIA cluster. A scheme to show the cluster geometry has been also drawn. The ρ profiles correspond to seven and four adjacent atomic rows in the basal (B rows) and type-I prism (P rows) planes, respectively. The label 0 indicates segment centre; the rows nearest a corner are 6 and 3 for B and P, respectively.

differences were found between atomic rows across the $(10\bar{1}0)$ slip plane, labelled P*m*. As an example we consider the rectangular 112-SIA cluster with shape factor $f = 0.48$. The results are plotted in semi-schematic form in Fig. 3(a) and (b) for the (0001) and $(10\bar{1}0)$ planes, respectively. For the sake of clarity, the Burgers vector density in both cases is plotted for only half of the atomic rows along a side. Fig. 3(a) shows clearly that $\rho(b)$ on the basal plane develops two maxima from row B5 next to the one at the corner (B6) to the one at the centre (B0), indicating that the dislocation core, with total Burgers vector $1/3[1\bar{2}10]$, is dissociated into two Shockley partial dislocations in the basal plane. The cluster side lying on the $(10\bar{1}0)$ plane in Fig. 3(b) exhibits only one maximum in $\rho(b)$ for all rows, revealing an undissociated dislocation core whose Burgers vector is $1/3[1\bar{2}10]$. The atomic structure described above is similar to that of smaller clusters reported earlier on the basis of simpler analysis of atomic structure [10,12].

The main features of the clusters in the PPII prism plane are summarised by the examples in Fig. 4. The plots in Fig. 4(a) illustrate the behaviour of $\rho(b)$ in the central part

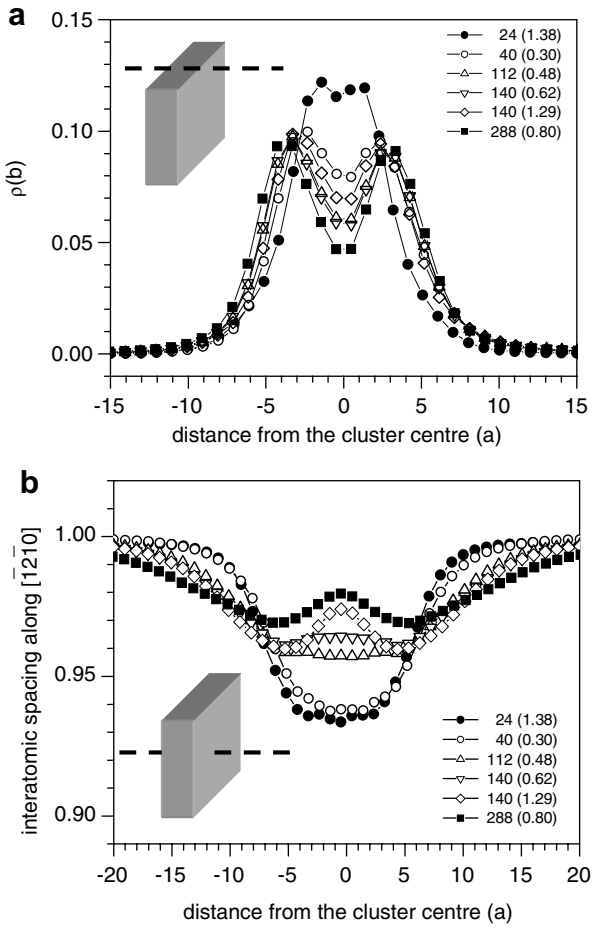

Fig. 4. (a) Profiles of $\rho(b)$ along atomic rows through the centre of a basal segment and (b) the interatomic spacing (relative to *a*) along rows through the cluster centre for rectangular clusters with different *n* and *f* values (shown in parentheses).

of the basal plane segment for clusters with different sizes and shape factors, and show that the same segment core structure is developed by all rectangular clusters. The clear presence of the two maxima for clusters containing 40 or more SIAs indicates the dislocation loop nature of the defect because they reveal the dissociated state of the core. Even for the smaller 24-SIA cluster there is a hint of two maxima, suggesting that dislocation character is partly developed in Zr for rather small clusters, as also observed for cubic metals [3]. The distance between the two maxima defines the spacing between the partials and is determined by the value of the I_2-type intrinsic stacking fault. The spacing increases with the number of SIAs from 2.5*a* for 24 SIAs to 7*a* for 288 SIAs, where *a* is the basal lattice parameter, and is almost independent of cluster size for more than about 100 SIAs. The latter spacing is consistent with recent computer simulation of the properties of an infinite, straight edge dislocation in Zr [14]. (The values of the energy of the I_2 basal fault and the PPI fault are 80 mJ/m^2 and 285 mJ/m^2, respectively, and the spacing of the Shockley partials for the basal edge dislocation is 8*a* [14].) The dissociation depends weakly on the shape factor, as can be seen for the two clusters of 140 SIAs having different *f* values for which the partial spacing is $\approx 6a$ in both cases. A similar study of $\rho(b)$ for rhombus clusters demonstrates that the dislocation core of the $\langle 10\bar{1}1 \rangle$ sides is not dissociated. The basal segments of hexagonal clusters are dissociated, however. By comparing these results with the binding energy data it is inferred that the formation of the I_2 stacking fault gives more stability to the clusters.

The atomic structure inside the crystal bound by the loop, i.e. inside the glide cylinder, is studied by plotting the variation of the interatomic spacing along the $[\bar{1}2\bar{1}0]$ axis of $\boldsymbol{b}$ through the cluster centre. These plots show the fluctuation in the atomic density along the crowdion direction and are presented normalised to *a* in Fig. 4(b) for the clusters selected in Fig. 4(a). There is a significant spread of the density fluctuation over a wide range along the axis. The maximum difference from the perfect crystal decreases with increasing cluster size: it ranges from 6% for the 24-SIA cluster to 3% for the 288 SIAs defect. The shape factor also affects the fluctuation (compare the plots for the 140-SIAs clusters with different shape factor). For large clusters the atomic spacing increases markedly towards the perfect value in the cluster centre (see the plots for the 288-SIA loop and the 140-SIA cluster with $f = 1.29$ in Fig. 4(b)).

The habit plane of the rectangular clusters changes towards the $\{10\bar{1}2\}$ orientation after annealing for a few picoseconds at temperatures as low as 150 K. The positions of atoms in two adjacent PPI planes projected onto a cross-section through the centre of the 112-SIA cluster annealed for over 330 ps at 150 K is presented in Fig. 5. The dissociated dislocation core structure is retained but there is relative shift of the partial positions in the upper (U) and lower (L) basal glide planes due to rotation of the habit plane away from the pure edge orientation. This feature has been also observed for clusters containing 80 and 168 SIAs and

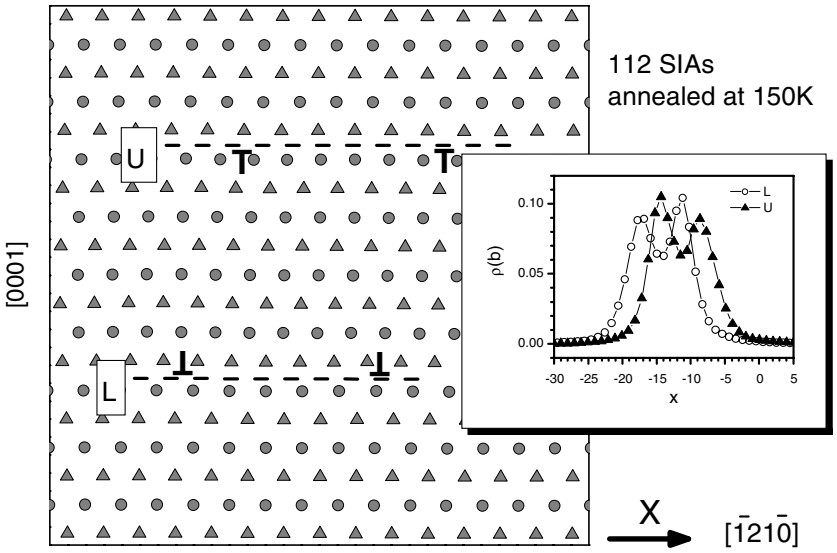

Fig. 5. $[10\bar{1}0]$ projection of atomic positions in two adjacent type-I prism planes through the centre of a 112-SIA cluster after 330 ps at 150 K and quenching at 0 K. The dislocation symbols and dashed lines indicate dissociation of the dislocation core on the basal plane. The inset shows $\rho(b)$ along the lines marked U and L.

is thought to arise from the elastic interaction of the (dipole-like) dislocation segments on the basal planes.

All the clusters in the PPI and PPII planes exhibit 1-D motion along the $[\bar{1}2\bar{1}0]$ direction at both 150 K and 1000 K. This motion arises from the crowdion nature of the individual SIAs. The resulting high mobility is restricted to the direction of $\boldsymbol{b}$ and has been analysed and reported previously for vacancy and SIAs clusters in Fe and Cu [1,2,4] and small SIAs clusters in Zr [12]. This motion results in displacement of atoms inside the glide prism relative to those outside. In irradiated metal, it would lead to enhanced interaction effects between a cluster and other defects lying in the vicinity of the glide prism.

3.2. Vacancy clusters

Complete relaxation to a 'collapsed' extended defect is generally observed only for large vacancy clusters. This is a general feature of simulations that use short-range, many-body interatomic potentials, as discussed earlier [2]. To avoid this problem we use the 'two-stage-relaxation' technique suggested in [2]. An initial configuration is first obtained by using only the pair part of the potential, which is repulsive and pushes atoms on either side of the vacancy platelet towards each other, thereby provoking collapse of the cluster, which is then relaxed with both the pair and many-body parts of the potential to ensure the final equilibrium configuration is achieved. All the results presented in this paper have been obtained by this method.

Clusters containing up to 271, 263 and 288 vacancies in the basal, PPI and PPII planes, respectively, have been considered. The clusters in the basal plane were hexagonal in shape whereas those in both prism planes were rectangular. As with the interstitial clusters, shape factors, f, of different value have been considered.

The cluster formation and binding energies, E_f and E_b, normalised to the total number of vacancies, n, are plotted as a function of n in Fig. 6. The energies presented for the PPI and PPII defects correspond to different values of f but, as reported above for SIA clusters, the influence of the shape factor is negligible for the energy scale considered and so the same symbols have been used for different configurations to enhance clarity. The binding and formation energies are very similar for the three habit planes for n up to approximately 150. For larger sizes the basal plane clusters are less stable and exhibit higher E_f than those in the prism planes. This is because of the presence of a stacking fault inside the collapsed defect – see below. Comparison of Fig. 6 for vacancies with Fig. 2 for interstitials shows that the formation energy of large vacancy and SIA clusters of the same size and shape is similar. This is evidence

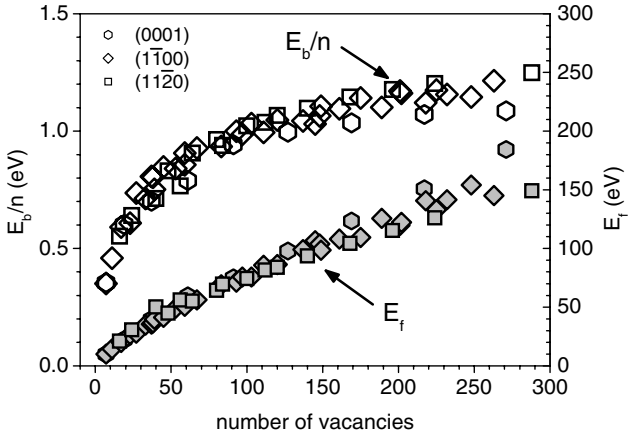

Fig. 6. Formation and normalised binding energy of vacancy in clusters vs. the number of vacancies n. Clusters created in the basal (hexagons) and the PPI and PPII planes (rectangles with different f) are considered.

that these clusters are essentially dislocation loops and their energy is mainly that of the dislocation segments that form their periphery, irrespective of the vacancy or interstitial nature. The binding energy of vacancy clusters, on the other hand, is significantly lower than that for SIA clusters of the same size. This is due to the much smaller reference energy, i.e. $E_f = 1.786$ eV, of the single defect used to calculate E_b. The difference in binding energy is important for the relative stability of clusters at high temperature in irradiated metal.

The cluster structure has been studied by analysing the atomic positions through the cluster centre in $[1\,0\,\bar{1}\,0]$ and $[0\,0\,0\,1]$ projections. The general finding for all clusters containing 48 or more vacancies in the PPII is that they have features characteristic of dislocation loops. They have Burgers vector $\boldsymbol{b} = 1/3\langle 1\,1\,\bar{2}\,0\rangle$ and are dissociated in the basal plane. As an example we show in Fig. 7 the Burgers vector distribution along the $[\bar{1}\,2\,\bar{1}\,0]$ atomic row through the centre of the loop segments in the $(0\,0\,0\,1)$ and $(1\,0\,\bar{1}\,0)$ planes for a cluster containing 112 vacancies. The dissociated core in the $(0\,0\,0\,1)$ plane is clearly seen from the presence of the two maxima. By comparing Fig. 7 with Fig. 3 it can be concluded that the dislocation structure is qualitatively the same as the one described in Section 3.1 for SIA loops created in the same habit plane. Quantitatively there are some differences in that the distance between the basal plane partial dislocations is smaller for vacancy loops, as can be seen by comparing the $\rho(b)$ profile for a SIA and a vacancy loop containing 112 defects in figs. 4(a) and 7, respectively; the distance between the partials is about $5a$ in the vacancy loop compared with about $6a$ for the SIA loop. Annealing loops with $n \geqslant 48$ at 700 K was found to retain the same dissociated loop configuration but slightly inclined to the pyramidal plane, as described above for SIA loops in the PPII plane.

Small clusters in the basal plane with $n \leqslant 61$ relax as faulted loops with stacking sequence ABAB · BABA. However, this is a metastable configuration that transforms into a lower energy state after annealing at 700 K for over 25 ps

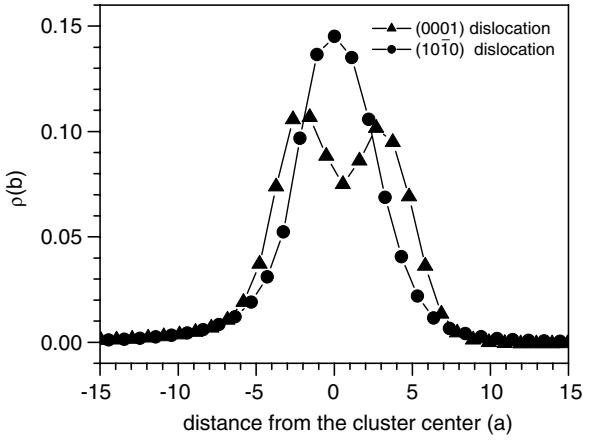

Fig. 7. Profiles of $\rho(b)$ along atomic rows through the centre of $(0\,0\,0\,1)$ and $(1\,0\,\bar{1}\,0)$ segments of a 112-vacancy cluster created in a PPII plane.

by a process in which the atoms in just one $(0\,0\,0\,1)$ plane adjacent to the fault (say plane B in the sequence above) shear to FCC-like positions (ABAB · CABA), forming an E-type extrinsic stacking fault. The resulting Burgers vector is $1/2[0\,0\,0\,1]$. (Since the atoms in only one plane are displaced, the process is formally equivalent to equal and opposite shears on adjacent planes – see, for instance, Fig. 6.4 of [15]). An example for a 61-vacancy cluster before and after annealing is depicted in Fig. 8, where the positions of the atoms in two adjacent $(1\,0\,\bar{1}\,0)$ planes are shown in a projection along $[1\,0\,\bar{1}\,0]$; the stacking sequence of closed-packed basal planes before and after annealing is at the side of the figure. It is clear that the atoms sitting in a B layer above the A sites occupied by vacancies are displaced to C positions, whereas those lying below keep their B positions, giving rise to the E-type fault. These defects are identified as the pyramid-like vacancy clusters found in simulation of displacement cascades [11]. The present results confirm that they are generated from agglomeration of vacancies in a basal plane, as pointed out in [6,11]. Larger clusters containing between 91 and 271 vacancies relax at 0 K to the stable E-fault configuration described above, i.e. $1/2[0\,0\,0\,1](0\,0\,0\,1)$ loops, and retain the same structure after annealing at 700 K over 600 ps. A simple estimate taking the energy for the E fault to be 1.5 times that for the I_2 fault shows that the contribution of the fault to the formation energy for large loops is about 0.1 eV per vacancy.

Clusters up to about 60 vacancies generated in the PPI plane relax as prismatic clusters with a structure similar to that described earlier [6,11]. The relaxed configurations of larger clusters depend on the shape and the number of vacancies in the two adjacent $(1\,0\,\bar{1}\,0)$ planes. They are found to be either faulted dislocation loops with $\boldsymbol{b} = 1/2\langle 1\,0\,\bar{1}\,0\rangle$ or perfect loops with $\boldsymbol{b} = 1/3\langle 1\,1\,\bar{2}\,0\rangle$ and habit plane $\{1\,1\,\bar{2}\,0\}$ or slightly inclined to it. The former configuration transforms to the latter by $1/6\langle \bar{1}\,2\,\bar{1}\,0\rangle$ shear upon annealing for about 150 ps at 700 K. An example of a perfect loop in shown in Fig. 9 for a cluster containing 156 vacancies.

3.3. Other issues

Experiments using electron microscopy have found that the damage developed during irradiation of zirconium consists of both vacancy and interstitial dislocation loops lying on prism planes of the hcp structure with Burgers vector $\boldsymbol{b} = 1/3\langle 1\,1\,\bar{2}\,0\rangle$, e.g. [16–18]. Loops large enough to be analysed experimentally contain hundreds of point defects and so the simulation results obtained here for large clusters are consistent with the observations. Experimentally, the stability of large vacancy loops is dependent on the temperature, for they are unstable at temperature above ≈723 K due to vacancy thermal emission. This is also consistent qualitatively with the simulation results that show that the binding energy per vacancy is <1.3 eV compared with up to 3.3 eV per defect in SIA clusters.

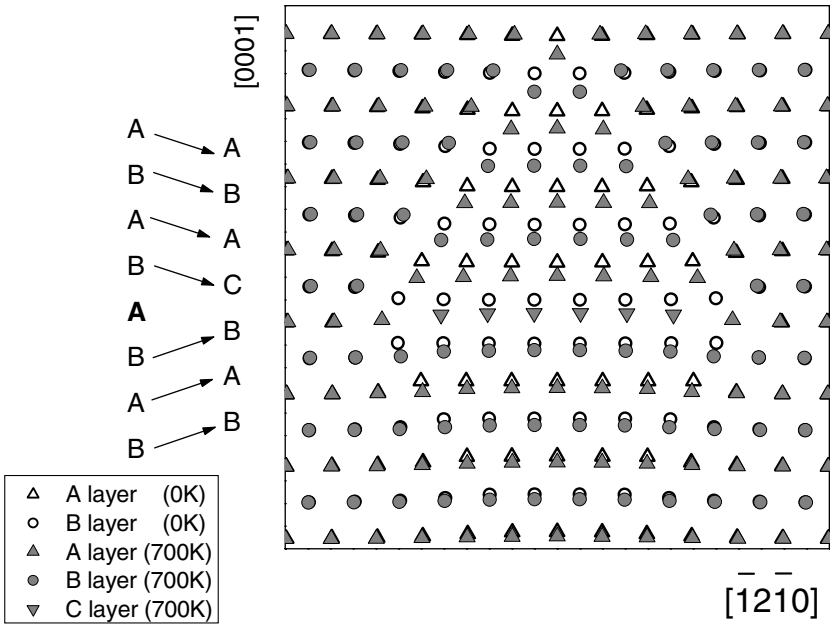

Fig. 8. Atomic structure of a 61-vacancy (0001) cluster in $(10\bar{1}0)$ projection at 0 K (open circles) and after annealing at 700 K and quenching at 0 K (grey symbols). The circles and triangles denote adjacent $(10\bar{1}0)$ planes. The corresponding sequence before (left) and after annealing (right) is given on the left to show the creation of an extrinsic stacking fault; the bold letter **A** corresponds to the layer removed to create the cluster.

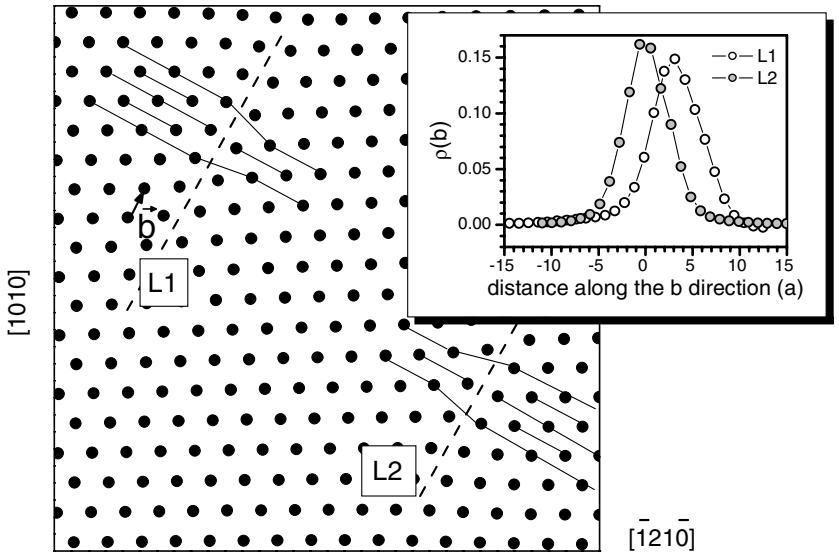

Fig. 9. [0001] projection of the structure of a 156-vacancy cluster created in the PPI. The inset shows the $\rho(b)$ variation along the L1 and L2 dashed lines.

Vacancy loops with (0001) habit plane and $\boldsymbol{b} = 1/3\langle 20\bar{2}3\rangle$ have been observed in zirconium and its alloys following neutron irradiation in the range 560–773 K. Basal loops of this type enclose an I_1- type intrinsic fault and may form from the ABAB·BABA collapse described in Section 3.2 by $1/3\langle 10\bar{1}0\rangle$ shear to ABAB·CBCB (see Fig. 6.4d of [15]). They were not found in the present work, possibly because this shearing process requires all the planes on one side of the fault to move, rather than just one for the E-type loop described in Section 3.2, and so much larger clusters are required for this to occur. Furthermore, the stability of faulted basal loops is believed to depend on the presence of solute elements that may lower the stacking-fault energy, and effects such as this cannot be treated with interatomic potentials currently available for Zr.

The interatomic potential used here also has limitations as far as simulation of pure Zr is concerned. The ratio of the basal and prism stacking fault energies, and the configuration of the single SIA, are known from recent *ab-initio* calculations [19–21] to be in error. Nevertheless, the potential has been widely used for defect studies and is considered to be the best currently available for a model hcp crystal having some Zr-like properties.

4. Conclusions

1. Rectangular interstitial clusters formed in the $\{1\,1\,\bar{2}\,0\}$ type-II prism planes, PPII, have a lower formation energy and higher binding energy than rhombic or hexagonal clusters in the same plane. The binding energy increases with the number, n, of interstitials in the cluster. SIA clusters with $n > 24$ PPI can be described as dislocation loops with Burgers vector $\boldsymbol{b} = 1/3\langle 1\,1\,\bar{2}\,0\rangle$. Side segments lying in the basal plane partly dissociate and enclose an I_2-type stacking fault. This dissociation helps to stabilise rectangular loops against other shapes.
2. Vacancy clusters lying in the prism planes have a lower formation energy and higher binding energy than clusters with the same number of vacancies in the basal plane. Clusters in prism planes with $n > 50$ have $1/3\langle 1\,1\,\bar{2}\,0\rangle$ dislocation loop character with a similar core structure to the interstitial clusters. Basal plane clusters relax to enclose an extrinsic E-type stacking fault in the habit plane. Larger ones ($n > 90$) have loop character with $\boldsymbol{b} = 1/2\ [0\,0\,0\,1]$.
3. The formation energy of stable vacancy and interstitial clusters of the same shape and size is similar whereas interstitial clusters have higher binding energy.
4. The results are qualitatively consistent with experimental findings reported elsewhere, e.g. [16–18]. They provide a quantitative framework for higher-order modelling using methods such as Monte Carlo simulation.

Acknowledgements

The research was supported by Spanish MCYT (MAT2002-04087-C02-02) and Universidad Complutense de Madrid (PR1/06-14445-A). It was partly sponsored by the Division of Materials Sciences and Engineering, US Department of Energy, under contract DE-AC05-00OR22725 with UT-Battelle, LLC.

References

[1] Yu.N. Osetsky, A. Serra, V. Priego, Mater. Res. Soc. Symp. Proc. 527 (1998) 59.
[2] Yu.N. Osetsky, D.J. Bacon, A. Serra, Philos. Mag. Lett. 79 (1999) 273.
[3] Yu.N. Osetsky, A. Serra, B.N. Singh, S.I. Golubov, Philos. Mag. A 80 (2000) 2131.
[4] Yu.N. Osetsky, D.J. Bacon, A. Serra, B.N. Singh, S.I. Golubov, J. Nucl. Mater. 276 (2000) 65.
[5] D.J. Bacon, J. Nucl. Mater. 159 (1988) 176.
[6] V.G. Kapinos, Yu.N. Osetsky, P.A. Platonov, J. Nucl. Mater. 195 (1992) 83.
[7] D. Kulikov, M. Hou, J. Nucl. Mater. 342 (2005) 13.
[8] V.G. Kapinos, Yu.N. Osetsky, P.A. Platonov, J. Nucl. Mater. 184 (1991) 125.
[9] S.J. Wooding, L.M. Howe, F. Gao, A.F. Calder, D.J. Bacon, J. Nucl. Mater. 254 (1998) 191.
[10] F. Gao, D.J. Bacon, L.M. Howe, C.B. So, J. Nucl. Mater. 294 (2001) 288.
[11] R.E. Voskoboinikov, Yu.N. Osetsky, D.J. Bacon, Nucl. Instrum. and Meth. B 242 (2006) 530.
[12] N. de Diego, Yu.N. Osetsky, D.J. Bacon, Metall. Mater. Trans. A 33 (2002) 783.
[13] G.J. Ackland, S.J. Wooding, D.J. Bacon, Philos. Mag. A 71 (1995) 553.
[14] R.E. Voskoboinikov, Yu.N. Osetsky, D.J. Bacon, Mater. Sci. Eng. A 400&401 (2005) 45.
[15] D. Hull, D.J. Bacon, Introduction to Dislocations, fourth ed., Butterworth-Heinemann, Oxford, 2001.
[16] A. Jostsons, P.M. Kelly, J. Blake, J. Nucl. Mater. 66 (1977) 236.
[17] M. Griffiths, J. Nucl. Mater. 159 (1988) 190.
[18] M. Griffiths, Philos. Mag. 63 (1991) 835.
[19] F. Willaime, J. Nucl. Mater. 323 (2003) 205.
[20] C. Domain, A. Legris, Philos. Mag. 85 (2005) 569.
[21] C. Domain, J. Nucl. Mater. 351 (2006) 1.